



Landslide susceptibility mapping using frequency ratio model: the case of Gamo highland, South Ethiopia

Leulalem Shano^{1,2} · Tarun Kumar Raghuvanshi³ · Matebie Meten¹

Received: 27 July 2020 / Accepted: 22 March 2021 / Published online: 29 March 2021
© Saudi Society for Geosciences 2021

Abstract

Landslide is the most frequently occurring geo-hazard in mountainous terrains of the world. It affects human life, infrastructures, landscapes, and human properties as well as their day-to-day activities. In the current study area which is found in the Gamo Zone of south Ethiopia, recurrent landslide hazards have occurred. To minimize this landslide hazard on human life and their properties, landslide susceptibility mapping is an important step for environmental planning. For this purpose, 1554 landslides and 9 landslide causative factors (both conditioning and triggering factors) were used. Each thematic layer has different classes and some of these classes influence landslide occurrence more than others. The most influencing factor classes which were identified by the frequency ratio model include slope classes between 12 and 45°; convex and concave classes of the curvature; aspect classes of north, northeast, south, and southwest directions; and elevation classes in between 2118 and 2492 m. The distance factors, proximity to streams, and lineaments 0–100 m and 0–200 m respectively have a very high on landslide occurrences. Land use/land cover factor has different classes and they have different levels of direct and indirect influences on landslide occurrences. The landslide susceptibility map was classified as very low, low, moderate, high, and very high classes each accounting for 17.8%, 29.19%, 28.55%, 17.52%, and 6.91% of the area respectively. To evaluate the reliability of this model, the landslide susceptibility map was verified using a receiver operating characteristic (ROC) curve with a value of 82% and through field observation. Therefore, this can be used by local, zonal, regional, and federal governments for land use planning, disaster prevention, and mitigation as it offers first-hand information.

Keywords Landslide susceptibility · Frequency ratio · Landslide inventory · Conditioning factors

Responsible editor: Zeynal Abiddin Erguler

✉ Leulalem Shano
leulalemshano@gmail.com

Tarun Kumar Raghuvanshi
tkraghuvanshi@gmail.com

Matebie Meten
matebe21@gmail.com

¹ Department of Geology, College of Applied Sciences, Addis Ababa Science and Technology University, Addis Ababa, Ethiopia

² Department of Geology, College of Natural Sciences, Arba Minch University, Arba Minch, Ethiopia

³ School of Earth Sciences, College of Natural Sciences, Addis Ababa University, PO Box 1176, Addis Ababa, Ethiopia

Introduction

Landslides are one of the most threatening disasters in mountainous terrain all over the world. They are considered as the most frequently occurring major hazards affecting human life, properties, infrastructures, and landscapes (Fell et al. 2008; Nguyen et al. 2019). To minimize this landslide disaster, different scholars have investigated different levels of studies in the different landslide affecting countries. In the current study area, there have been landslide hazards and risks in some parts of Shafe and Baso catchments, south Ethiopia. Prior to this study, there was no landslide study in these two catchments. To minimize the landslide risk, the landslide susceptibility study is one of the basic components of the landslide study which was applied in the present study areas. In the last 30 years, the population growth has increased in these catchments that create new settlers around high and very landslide susceptible areas which expose people, properties, and infrastructures to landslide hazards.

During landslide studies, there are different terms such as landslide inventory, landslide susceptibility, landslide hazard, and landslide risk have been commonly used. These all terms are their own applications, data types, stages of studies, mapping scales, and purposes. From these different terms, landslide susceptibility and hazard study are the most confusing terms. They have standards but most researchers have not used them separately rather they use them interchangeably. However, as described in AGS (2000), Guzzetti et al. (2005), van Westen et al. (2008), and Reichenbach et al. (2018), their differences were well defined. Based on these definitions, landslide susceptibility is the probability of potential occurrence of slope failure, given a set of geo-environmental conditions. Or landslide susceptibility measures the degree to which a terrain can be affected by future slope movement (Reichenbach et al. 2018). As shortly explained in (Guzzetti et al. 2006), it is an estimate of “where” landslides are likely to occur. On the other hand, landslide hazard study includes “where” landslides are likely to occur (susceptibility component) and also estimates the time “when” the landslide occurs as well as how frequently it occurs (Guzzetti et al. 2005; Reichenbach et al. 2018). The current study was considered the landslide susceptibility mapping according to the above definitions.

In the landslide studies, there are two broad approaches (qualitative and quantitative) with several sub-groups. For both approaches, landslide studies may use the same methods with different landslide data types and considerations. As discussed in different literature (Aleotti and Chowdhury 1999; Guzzetti et al. 1999; Ruff and Czurda 2008; Raghuvanshi et al. 2014; Lee 2015; Reichenbach et al. 2018; Shano et al. 2020), the qualitative approaches (heuristic, landslide inventory, geomorphological approaches) evaluation of actual landslides compared with characteristics of geomorphology or geology (e.g., Guzzetti et al. 1999; Ayalew and Yamagishi 2004; Dahl et al. 2010; Stanley and Kirschbaum 2017). These methods are strongly dependent on the experience of the surveyors, but they are the only practicable approach for landslides caused by different mechanisms. Based on the scale of study these approaches are applied in all scale ranges (Aleotti and Chowdhury 1999; Shano et al. 2020). The quantitative approach is grouped into different categories such as deterministic or mechanical methods that were applied by various researchers (e.g., Sarkar et al. 2016; Ciurleo et al. 2017; Krušić et al. 2017; Shano et al. 2020) and statistical (e.g., Carrara et al. 1991; Jager and Wiczorek 1994; Donati and Turrini 2002; Zhou et al. 2002; Meten et al. 2015; Berhane et al. 2020) and machine learning/artificial intelligent (Catani et al. 2005; Pradhan and Buchroithner 2010; Pradhan 2013; Ada and San 2017; Kavzoglu et al. 2018; Hu et al. 2020; Kalantar et al. 2020a; Shano et al. 2020; Wang et al. 2020). Some of the researchers also used hybrid types of approaches (artificial intelligence with statistical methods) for landslide

analysis (Chen et al. 2018; Li and Chen 2019; Nguyen et al. 2019). Deterministic method is not applicable in regional-scale landslide susceptibility analysis due to non-extrapolation of mechanical data on a small scale and difficulty to collect geotechnical data from large areas. It is favorable for large-scale engineering design purposes. Statistical approaches are mostly applied for medium and upper margin of small-scale mapping or susceptible areas in shallow landslides. Machine learning/artificial intelligence uses some statistical assumptions which are applicable when there is no mathematical relation between cause and effect (Chowdhury and Sadek 2012; Shano et al. 2020).

For the current study, the frequency ratio model was selected for landslide susceptibility mapping of the area. This model is more accurate to map landslide susceptibility classes in each thematic layer (Hong et al. 2015; Meten et al. 2015; Rahardianto et al. 2017; Khan et al. 2019; Silalahi et al. 2019; Berhane et al. 2020). It is one of the most widely applied bivariate statistical approaches for landslide susceptibility mapping. The occurrence of landslides in the current study area is mainly related to geological, hydrological, geomorphological, climatic, and anthropogenic factors that lead to a wide variety of slope instabilities. Besides, the problems such as misusing landslide susceptibility and hazard, other problems related to landslide studies include a random selection of independent factors, use of inappropriate mapping scale, purpose, and incomplete landslide inventory. However, a selection of landslide influencing factors is the most basic issue to evaluate the real condition either of landslide susceptibility or landslide study. That is needed for a critical field evaluation and/or image analysis to select the influencing predisposing factors. Therefore, this study has applied the principles of GIS-based frequency ratio model following the concept of landslide susceptibility principles; identified the landslide conditioning factors of the area based on field evaluation; and detailed landslide inventory throughout the study area.

The study area

The study area is located in southern Ethiopia (Fig. 1), western escarpment of the East Africa rift system. At the base of this escarpment, there are two lakes namely Abaya and Chamo. The area is accessed in two ways, one is from Arbamich to Merab Abaya passing through asphalted road about 40 km and then about 2 km to the north and finally return to west 23 km seasonally gravel road. The elevation of the area ranges from 1212 to 3046 m and the two lakes have an elevation of about 1000 m, and the height mountain is 3046 m. The second option is from Arbaminch through Chencha to Bribir of all weathered roads with a total distance of about 64 km.

The geology and tectonic setting of the study area are simple and identifiable although the area is tectonically active.

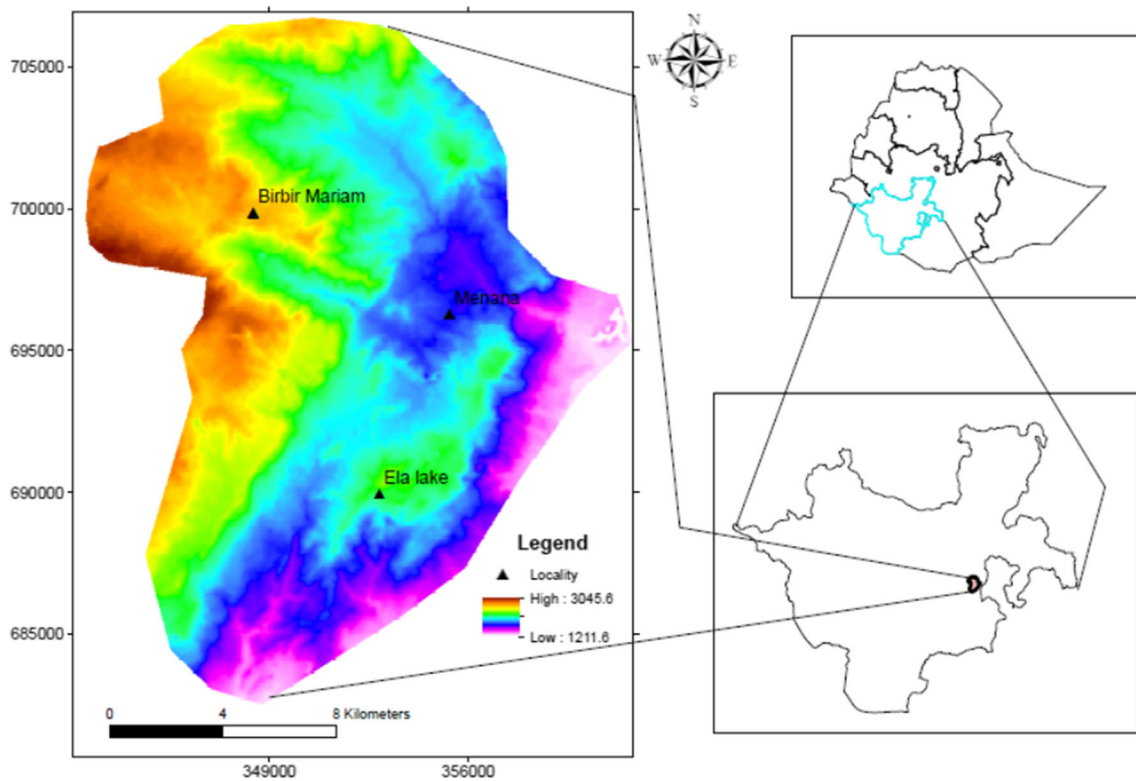


Fig. 1 Location map of the study area

The area is covered by four lithological units; these are basalt, ignimbrite, rhyolite, and tuff. Mostly the area is covered by basalt, which is characterized as highly weathered and fractured. The ignimbrite is highly fractured but less weathered and covers flat areas with some steep cliffs. The areal coverage of rhyolite and tuff is very small; rhyolite is found in the eastern parts of the study area and the tuff northern part of the study area. There are tectonic relics in the area with north-south and northeast to southwest oriented major faults. These faults are visible in between ignimbrite and basalt units and also within basalt.

Data types and method

Remote sensing and field data

The Advanced Spaceborne Thermal Emission and Reflection Radiometer (ASTER)-derived digital elevation model (DEM) with a spatial resolution of 30×30 m was used to generate geo-morphometric parameters of the study area. These geo-morphometric parameters are slope, aspect, curvature, and elevations. Land use/land cover map was derived by using sentinel images of different bands with various resolutions. Geological and stream maps were produced by geo-referenced with the aid of Ethio-top sheet nos. 0637 D1, D2, and D3 and field surveys.

Landslide inventory

Landslide inventory maps may be prepared by using remote sensing techniques and/or field surveys. These are the cardinal data collecting techniques for landslide susceptibility mapping (e.g., van Westen et al. 2013; Murillo-García et al. 2014; Nhu et al. 2020; Kalantar et al. 2020b). Landslide inventory is the principal input data for landslide susceptibility mapping. The present study used landslide scars from Google Earth pro image and field survey to collect data. A total of 1554 landslides were collected by using the abovementioned methods. From 1554 landslides, only 65 were used for classification or landslide type analysis purposes because these 65 landslides are more or less active to identify the types of landslides. As of 65 active landslides, 60% (39) are debris while 25% (16) and 15% (10) are earth and rock, respectively.

Landslide causative factors

The spatial distribution of landslides is depending on different environmental and triggering factors. To identify those factors, there should be detailed remote sensing image analysis and field surveys. After a detailed assessment, nine causative and one triggering factor were selected for first stage analysis. Those factors are slope, aspect, curvature, elevation, geological units, proximity to lineaments, proximity to stream erosion, groundwater, land use/land cover, and rainfall. From

these factors, groundwater manifestation was discussed in the text but no map due to subsurface data limitation. In the second stage of data analysis, all other predisposing factors and a triggering factor are highlighted in the following sub-topics and will be discussed in result and discussion sections as well.

Slope

The slope gradient is the most influential factor which directly influences soil water content, soil formation, erosion potential, and slope stability (Riaz et al. 2018; Berhane et al. 2020) (Fig. 2c, f). It is a major factor for slope instability and landslide as a higher slope angle equates to higher shear stress and a greater tendency to fail if the materials are soil and weak rocks (Abija et al. 2019). In this study, slope gradient was classified into five classes. These are 0–5°, 5–12°, 12–30°, 30–45°, and >45°. This classification is indicated (Fig. 3a), on a slope map. Some rockfalls have been observed with slope gradients greater than 45°. These types of slopes are found on ignimbrite rock units while most scars of normal faults in the area have angles greater than 45°.

Aspect

Aspect indicates the direction of slope face (0 to 360°). It is reducing the sunlight to effectively heat the ground which saves the moisture content of the soil (Akgün and Bulut 2007; Park and Kim 2019; Wubalem and Meten 2020). In this research, aspect was classified into ten categories like flat (–1°), north (N), northeast (NE), east (E), southeast (SE), south (S), southwest (SW), west (W), and northwest (NW). If the area is covered by the shadows of curvature, on the accumulated rainwater, additional rainfall is added; such types of conditions highly enhance the probability of landslide

occurrence (Erener et al. 2016; Wubalem 2021). As identified, the most influencing aspect directions are north, northeast, southeast, southwest, and west directions (Fig. 3b).

Curvature

In the curvature map, large negative indicates concave, zero, and both sides near to zero reveal a flat surface and large positive indicates the convex slope of the area. Slope curvature is related to erosion and groundwater accumulation of the area (Neuhäuser and Terhorst 2007; Weirich and Blesius 2007; Wang et al. 2009; Riaz et al. 2018; Wubalem 2021). If the curvature is concave there is a high probability of groundwater occurrence and this groundwater has its own influence on slope instability. But if the slope curvatures of the area are convex in shape, this made favorable conditions for the erosion of the area. Thus, erosion is the dominant factor of the study area which influenced the slope instability. The field observation showed that both concave and convex slopes are composed of soil and highly weathered rock units. This is also assured in Fig. 3d; the convex class is highly influencing landslide as compared to concave class.

Elevation

According to a DEM obtained from the Advanced Spaceborne Thermal Emission and Reflection Radiometer (ASTER), the elevation of the study area varies from 1000 to 3046 m. The DEM map of the study area was classified into four classes (Fig. 3c), with these classes landslide training data was combined for landslide analysis. Elevation has an indirect influence on slope instability or landslide by affecting the rainfall amount and vegetation coverage. Due to this elevation

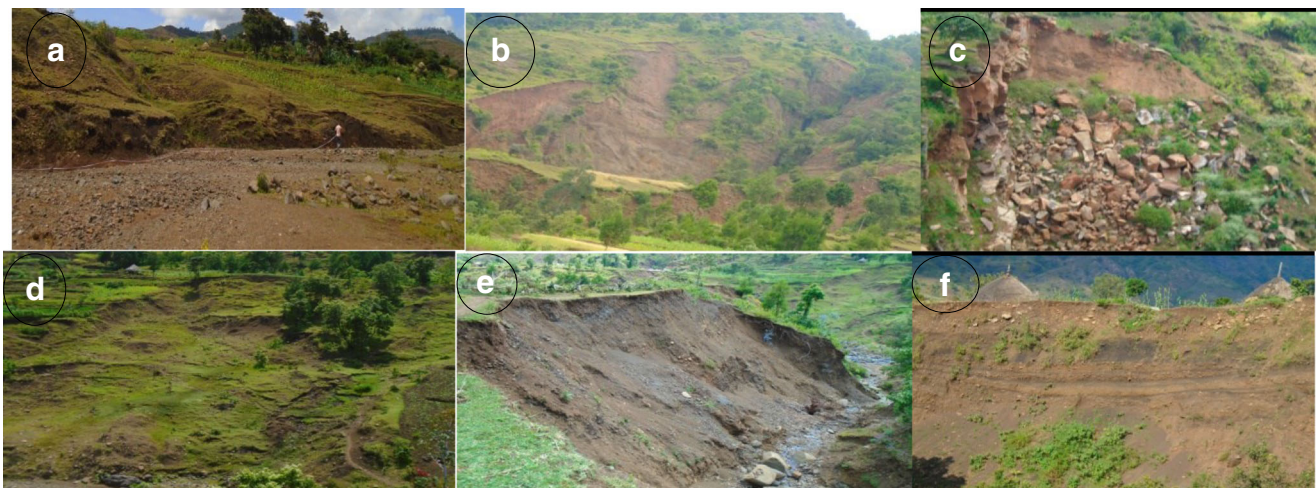


Fig. 2 Selected field photographs showing types and characteristics of landslides, **a** creep type of landslide due to stream erosion and shallow groundwater; **b** landslides on sparsely vegetated, sloppy area; **c** rock slide

on ignimbrite rock on sloppy area; **d** rotational landslides on highly weathered basaltic rocks; **e** landslides due to toe erosions; **f** landslide on alluvial soil around the banks of streams

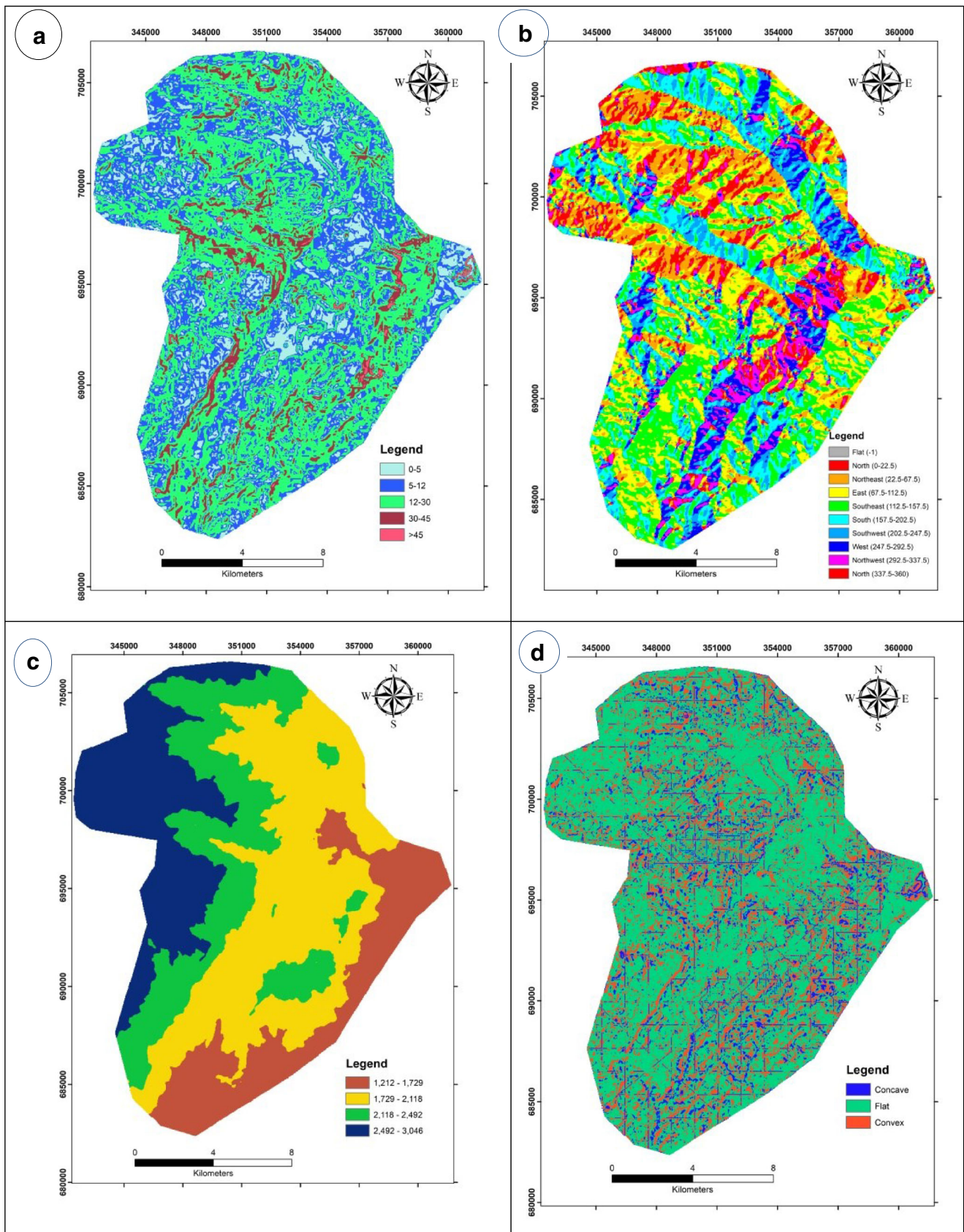


Fig. 3 a Slope map in degree, b aspect direction in degree, c elevation in metre, d curvature map, e proximity to lineaments in metre, f proximity to streams in metre, g lithology map, h land use/land cover map

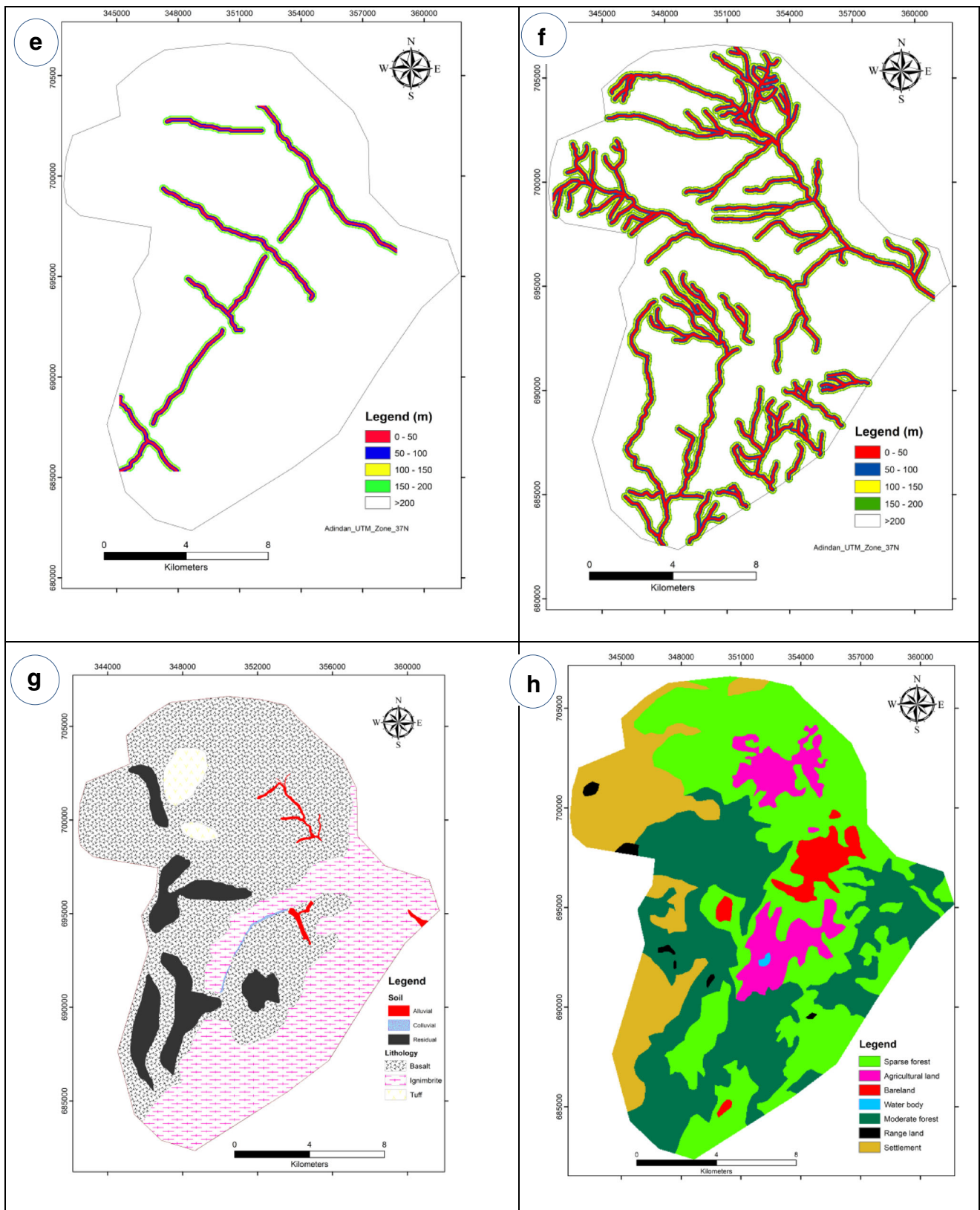


Fig. 3 (continued)

variation, annual rainfall at a lower elevation ranges from 400 to 1200 mm and at an upper elevation from 560 to 2300 mm.

Lithology

The lithology of the study area consists of both rocks (tuff, ignimbrite, and basalt) and soils (residual, colluvial, and alluvial) (Fig. 3g) that have different engineering properties. Lithology is one of the landslide causative factors (Riaz et al. 2018; Berhane et al. 2020). When the rock unit is loose and fragile, the probability of landslide occurrence will increase. The study area is covered dominantly by two lithologic units (basalt and ignimbrite) from which basalt covers 60% and ignimbrite 30%. Basalt is found in the cliff and mountain part of the study area. It is highly fractured and weathered and it is difficult to characterize basalt because most of the basalts are extremely fractured and weathered. Ignimbrite covers the flat land and some steep slopes of the study area. It is moderately fractured and slightly weathered. By visual inspection, the soil of the study area consists of silt, sand, and gravel along stream channels and banks. At the foot of the mountain, there are mixed colluvial and alluvial soils. At the top of the mountain and flat plateau land, residual soil that contains fine-grained soils and rock fragments was encountered.

Proximity to lineaments

Lineament geometry and fault rupture have a direct influence on the distribution of landslides (Mahmood et al. 2015; Riaz et al. 2018). The lineaments of the areas were identified from the ASTER image with a resolution of 15 m × 15 m and were checked during field surveys. These lineaments were delineated on this image and exported into ArcGIS10.4. The Euclidean distance method was applied in the ArcGIS environment to buffer lineaments into a distance to lineament thematic layer of five classes, i.e., 0–50 m, 50–100 m, 100–150 m, 150–200 m, and >200 m (Fig. 3e). These buffering distances were fixed based on Google image interpretation and field observation. In general, landslide density decreases as the distance to lineament increases (Table 1).

Proximity to stream erosion

Streams/rivers facilitate slope failures/landslides by eroding the supporting geological materials, increasing the moisture content, and increasing groundwater level (Berhane et al. 2020) (Fig. 2a, e). There are two small rivers that receive water flow from very small tributary streams. These small rivers are named the Mezo and Shafe Rivers. The Mezo River starts from the southern part of Birbir towards the rift center. The initial points of both rivers are very rugged topography and very small streams which start from very rugged topography towards flat land. When these streams flow from initial points

to the rift floor, there are lots of river incision, erosion, and land sliding. When the flow of streams is concentrated from original points towards these rivers, the eroding power will increase which may initiate landslides. From the lower parts of the study area, the slope gradient decreases as the eroding power of streams decreases. Mostly, landslides are concentrated near the stream channel in steep slope areas. A buffering analysis was carried out on streams using Euclidean distance buffering in ArcGIS to classify the distance to stream factor into five classes of 0–50 m, 50–100 m, 100–150 m, 150–200 m, and > 200 m (Fig. 3f). The frequency ratio value was greater than 1 in the distance to stream class of 0–50 m indicating the highest probability of landslide occurrence in this class (Table 1).

Land use/land cover

Anthropogenic factors are human activities-related factors and other living things that affect the environment. In this research, the land use/land cover factor is categorized into seven groups. These are settlement, agricultural land, grazing land, bare land, waterbody, moderate forest, and sparse forest (Fig. 3h). The anthropogenic factor is one of the conditioning factors that bring the slope stability to a marginal point of sliding. Human beings are destroying their environment and are destroyed by their environments. For example, they destroy plants and grasses and divert stream channels in turn these initiate erosion and landslide. During fieldwork and remote sensing image interpretation, these are visible activities and processes. The settlement number increases and the destruction of trees highly expanded. As a result, several gully erosion facilitated shallow landslides in the present study area. As described in (Shu et al. 2019; Mersha and Meten 2020) land use/land cover is the most influencing factor for rainfall-triggered landslides.

Groundwater

Groundwater is one of the internal initiating conditioning factors for deep landslides (Fig. 2a, d). It facilitated the occurrence of landslides with a failure surface greater than 5 m (Ayalew 1999; Van Asch et al. 1999; Nhu et al. 2020). This groundwater is initiating landslides by developing pore water pressure within geological material, lubricating failure surfaces, and increasing stress on failure surfaces. Most landslides in the current study area were identified around flowing springs thereby developing a failure surface. Majorities of landslides that occurred due to groundwater influences are debris and earth flows which were found in Layo triga, Manana, and Done localities. Some failure surface exposures revealed that sliding taking place when the groundwater flows from fractured rock to soil layer due to

Table 1 Frequency ratio values of each class of all thematic layers

Factor	Class	Pixclass	%class	Pixell and sl	%landslide	FR
Slope (degree)	0–5	35,267	11.3	317	4.61	0.41
	5–12	98,486	31.5	1348	19.61	0.62
	12–30	151,182	48.4	4045	58.84	1.22
	30–45	25,799	8.3	1139	16.57	2.01
	>45	1861	0.59	26	0.38	0.64
Aspect (degree)	Flat (-1)	37	0.012	0	0	0
	0–22.5	18,220	5.83	660	9.6	1.65
	22.5–67.5	42,895	13.72	1352	19.67	1.43
	67.5–112.5	56,750	18.15	985	14.33	0.79
	112.5–157.5	63,840	20.42	936	13.61	0.67
	157.5–202.5	46,145	14.76	1097	15.96	1.08
	202.5–247.5	29,105	9.31	873	12.70	1.36
	247.5–292.5	23,069	7.38	284	4.13	0.56
	292.5–337.5	19,417	6.21	342	4.97	0.80
	337.5–360	13,117	4.20	346	5.03	1.20
Elevation (m)	1212–1729	53,419	17.09	184	2.68	0.16
	1730–2118	116,531	37.28	2234	32.49	0.87
	2119–2492	73,492	23.51	3069	44.64	1.90
	2493–3046	69,153	22.12	1388	20.19	0.91
Curvature	Concave	157,254	50.31	3453	50.23	1.05
	Flat	4264	1.36	80	1.16	0.85
	Convex	151,077	48.33	3342	48.61	1.21
Proximity to stream (m)	0–50 m	17,885	17.83	807	31.95	1.79
	50.1–100 m	25,659	25.58	648	25.65	1.00
	100.1–150 m	26,959	26.88	651	25.77	0.96
	150.1–200 m	29,809	29.72	420	16.63	0.56
Proximity to lineament (m)	0–50 m	4408	19.90	198	24.91	1.25
	50.1–100 m	5562	25.12	233	29.31	1.17
	100.1–150 m	5977	26.99	189	23.77	0.88
	150.1–200 m	6199	27.99	175	22.01	0.79
Geological units	Basalt	188,514	61.86	5429	79.00	1.28
	Ignimbrite	7296	2.39	263	3.83	1.60
	Tuff	28,520	9.36	513	7.465	0.80
	Residual soil	2266	0.74	69	1.00	1.35
	Colluvial	77,738	25.51	556	8.09	0.32
	Alluvial	391	0.13	42	0.61	4.76
Land use/land cover	Agricultural land	99,708	32.72	2675	38.93	1.20
	Water body	257	0.084	0	0	0
	Bare land	3001	0.985	78	1.135	1.15
	Sparse forest	96,685	31.73	3373	49.1	1.55
	Moderate forest	33,645	11.041	40	0.582	0.05
	Range land	1215	0.39872	0	0	0
	Settlement	71,102	23.33317	708	10.30	0.44

increment of pore pressure. As described above, some deep landslides are near Mezo stream and at north-eastern part of Birbir, due to more than 10 houses being demolished and 80 people displaced.

Triggering factor

The rainfall is the most frequently triggering factor of landslide in most mountain terrains globally. It is initiating the

landslides from the marginal point to sliding the geological materials in the different slope levels. In the present study area, the most triggering factor is prolonged and heavy rainfall. Almost all landslides have occurred in the area due to prolonged rainfall. In this Gamo Mountain Chain, the monthly and annual minimum and maximum rainfall are 35 to 180 mm and 580 to 2400 mm, respectively. In addition to rainfall, there is earthquake occurrence but there is no archived earthquake catalog data with respect to landslide occurrence in the study area. Hence, the frequency ratio model that was applied in this study did not consider earthquake as a triggering factor but rainfall was considered as a triggering factor in the analysis.

Landslide susceptibility

The landslide susceptibility is the spatial propensity of the slope. For this analysis, the first step was to collect the landslide inventory data with the aid of Google Earth image and field survey. The analysis was done by using the frequency ratio approach (Hong et al. 2015; Rahardianto et al. 2017; Khan et al. 2019; Silalahi et al. 2019). Based on this frequency ratio model, the area was classified into five susceptibility classes of very low, low, medium, high, and very high. During this analysis, different landslide areas and influencing factors were associated and analyzed. These include geologic (lithology and soil type), morphometric (slope gradient, aspect, curvature, and elevation), distance (proximity to lineament, and proximity to stream), land use/land cover, and hydrological (groundwater, and rainfall) factors which were selected for susceptibility analysis.

Frequency ratio

This research was used for landslide susceptibility analysis by applying a statistical approach, frequency ratio. For landslide analysis or zonation by frequency ratio method, it needs all maps in raster format. The basic software, the current research applied was ArcGIS and Microsoft excel. All maps were prepared in the same format, same coordinate, projection system, and same pixel size; in this case, 30-m×30-m pixels were used. After preparation of all the selected factors in these formats, the frequency ratio analysis was applied. These maps have different formats such as vector and raster maps. Vector maps in this research are lithologic, land use/land cover, lineaments, streams, and landslide inventory maps. Raster maps are those maps derived from DEM data. Those maps in the form of vectors or polygons/points should be rasterized before being used in the frequency ratio model. To rasterize those maps, the conversion tools to raster format were used.

In short, to produce the landslide susceptibility map by using the frequency ratio model, there are nine basic steps followed. These are (1) landslide inventory map preparation, (2) different factor map preparation; (3) rasterization of some

of the maps initial not in the form of raster; (4) reclassifying all factor maps; (5) integrating each factor map with landslide training map/inventory map; (6) calculating the frequency ratio of each factor map; (7) encoding all factor maps with frequency ratio values; (8) by summing up all factor maps together on Map algebra; and (9) finally, reclassify into different susceptibility classes. This research applied these all steps and produced the landslide susceptibility map by using the frequency ratio model. When we use any familiar statistical method, the difficulty is not about understanding the concepts behind them but narrating all the steps to be followed sequentially. This frequency ratio model is one of the statistical methods that underwent through all the aforementioned steps to produce a landslide susceptibility zonation map. Before classifying the landslide susceptibility map, the summation of frequency ratio raster maps should be done as indicated in step 8 above.

Thus, a frequency ratio for a parameter class greater than one shows a strong correlation for landslide occurrence whereas a frequency ratio less than one indicates a low correlation of the factor class with the landslides (Lee and Min 2001; Chimidi et al. 2017; Mersha and Meten 2020). The frequency ratio (FR_d) can be expressed as Eq. 1:

$$FR_d = \frac{\%Ls}{\%Am} \quad (1)$$

where “ FR_d ” is the frequency ratio for the causative factor class, “ $\%Ls$ ” is the percentage of landslides in a causative factor class, and “ $\%Am$ ” is the area of the causative factor class as a percentage of the entire map.

Furthermore, the landslide susceptibility index (LSI) for each pixel is the summation of total overlapped pixels and is given by Eq. 2:

$$LSI = \sum_{d=1}^n FR_d \quad (2)$$

If the LSI value is high the landslide hazard is considered to be high. The LSI can also be represented as the landslide hazard index (LHI) (Pradhan and Lee 2009; Pradhan et al. 2010; Shano et al. 2020).

Result and discussion

Landslide inventory analysis

Landslide inventory is a collection of landslide scars or distribution by using remote sensing images or/and field observations. It is the simplest form of landslide mapping if there were archived landslide data. However, the collection of landslide inventory is somewhat difficult from multi-temporal image analysis to know the series of landslide occurrence within the specific time. This landslide inventory map is classified

into different categories based on purpose, scale, length of time for investigation, the budget allocated for investigation, and type of investigation (landslide susceptibility or hazard). Based on the type of mapping, the landslide inventory map can be classified as an archive or geomorphological inventory (Guzzetti et al. 2000; Malamud et al. 2004; Guzzetti et al. 2012). An archive inventory shows the information on landslides that were taken from different literatures or other archive sources (e.g., Taylor and Brabb 1986; Guzzetti et al. 2012; Dagdelenler et al. 2020). In the present study area, there was no literature or other archive sources to be used in the analysis. Due to this, the current study did not use such type of information. The second category is geomorphological inventories which can be divided into historical, event, seasonal, or multi-temporal inventories (Guzzetti et al. 2012). This research used historical and seasonal landslide scars for landslide inventory due to lack of event or archived datasets.

The main importance of landslide inventory map is the past landslide used to predict the future landslide occurrence; to know the location or density of landslide; to identify the mechanism of failure; and to validate landslide hazard and risk maps (Varnes and IAEG 1984; Carrara et al. 1991, 1995; Erener and Düzgün 2011; Kalantar et al. 2020b). According to van Westen et al. (2005), the spatial data for landslide susceptibility, hazard, and risk analysis are mainly grouped into four. These are landslide inventory data, environmental factors, triggering factors, and element at-risk data. Of these, the landslide inventory is considered to be the most important data because it reveals the location of landslide phenomena, the types, failure mechanisms, causal factors, frequency of occurrence, volumes, and the damage that has been caused.

Furthermore, a landslide inventory is an important component of the spatial database, which records the details of the existing landslides and helps in the analysis of the connections between landslides and influencing factors. Therefore, in this research, the past and current landslides have been identified from Google Earth image interpretation and field observation (Fig. 4). This research selected polygon-based inventory as it contains not only landslide initiation areas but also run-out areas, including valleys that had been affected by debris flows and areas that are prone to landslides as stream banks, cuts slopes, and cliffs.

This inventory map of the area reveals that landslides are concentrated in the areas which are closer to lineament or fault, river banks, and sloppy areas. According to the size of the landslide, large-scale landslides occurred in the Zalagutisha kebele, Layo tirma, and Birbir villages. In these areas, the relics of old landslides were clearly observed. In general, a series of large-scale landslides have occurred in these areas.

For this analysis, the landslide inventory map was systematically divided into two groups which constituted training data 70% and testing datasets 30%.

Landslide causative factor analysis

The selected landslide causative factors include geomorphometric factors (slope gradient, aspect, curvature, and elevation), geologic units (lithology and soil types), distance factors (proximity to lineament and streams/rivers), groundwater, land use/land cover, and rainfall (Riaz et al. 2018; Mersha and Meten 2020; Wubalem 2021). To evaluate these factors, the result of the frequency ratio values of each factor class in each thematic layer was used. Eight predisposing and one triggering factor with landslide inventory of different classes were prepared (Fig. 5(a–h)) to be analyzed using the frequency ratio model. The eight finally selected factors have their own level of influence on the slope stability of the study area. These levels of influence are revealed in Table 1 and Fig. 5.

Morphometric factors are one group of landslide influencing factors that are identified in this research work. These factors include slope curvature, slope gradient, slope aspect, and elevation. When the researcher used the frequency ratio model for landslide susceptibility analysis, it focused to identify the effect of the various classes within each thematic layer. For instance, the slope curvature was classified into three classes, namely concave, flat, and convex. The concave class has a negative value which indicates that from both sides of the slope curvature surface and local groundwater flow towards one direction and is influenced by accumulated water in the concave area. This accumulated water develops groundwater pressure and initiates landslide occurrence (Van Asch et al. 1999; Duman et al. 2005; Riaz et al. 2018). There are many landslides that have occurred in the central, southwestern, and northern parts of the present study area under this condition. The influence of concave slope is represented in Fig. 5a, which however showed that the convex-shaped slopes have a greater degree of influence as compared to the concave ones.

In the flat curvature, there is no significant landslide occurrence that is registered to mention in this type of area. As indicated in Fig. 5a, the landslides were initiated in the convex parts of the slope curvature due to erosion. In profile curvature, both concave and convex slopes are considered as conditioning if the area is composed of soils and/or highly weathered rocks. It affects the acceleration and deceleration of downslope flows, which is the result of erosional and depositional processes, causing landslides (Wang et al. 2015; Pal and Chowdhuri 2019).

The slope gradient is an essential component of the landslide influencing factor set which indicates how steep the ground surface is. The slope has a range between 0 and 90°, which correspond to the flat and vertical slopes, respectively. In the study area, the minimum slope angle is 0°, and the maximum of 79°. Slope angle is classified into five classes of 0°–5°, 5°–12°, 12°–30°, 30°–45°, and greater than 45°. From these four classes, the most landslide influencing classes

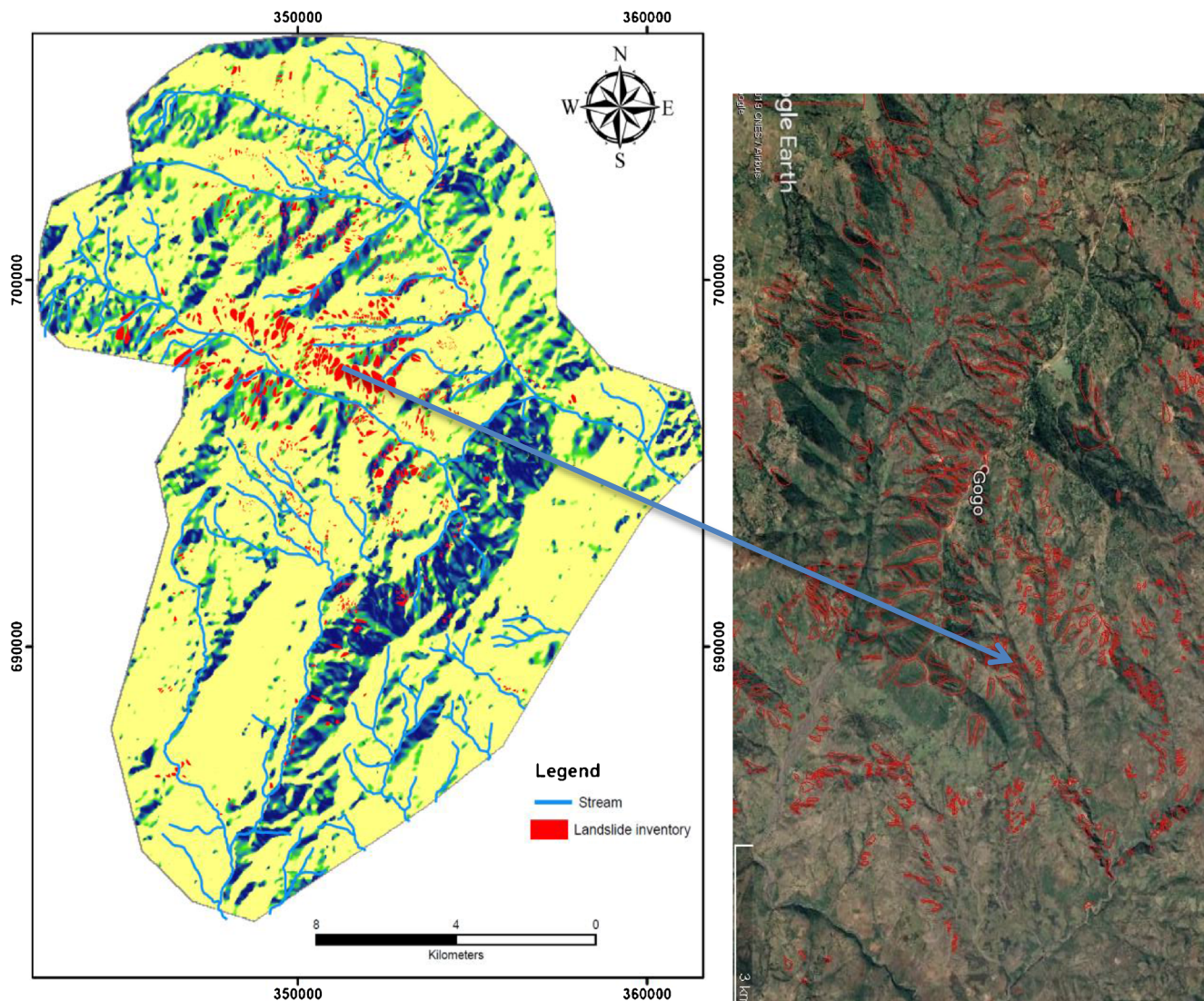


Fig. 4 Landslide inventory maps that reveals the spatial distribution of landslide

are 12° – 30° and 30° – 45° that are indicated in Fig. 5b. The materials in these slope classes are composed of different types of soils and highly weathered and fractured rocks which decrease the shear strength of these geological materials.

The slope aspect is one of the most influencing factors of slope instability (Budimir et al. 2015; Abdulwahid and Pradhan 2017). It affects the slope's exposure to sunlight, wind, and rainfall thereby affecting the weathering of rock and the moisture content of the geological materials. The aspect map of the study area was classified into ten classes of flat, north, northeast, east, southeast, south, southwest, west, northwest, and north (Fig. 5c) among which the north, northeast, south, and southwest aspect classes the most landslide-prone classes.

Elevation in the study area, which ranges from 1212 to 3046 m, affects the vegetation cover and the amount of rainfall. Some studies argued that soil texture is commonly related to elevation in which finer materials are found in the

downstream (lowland) areas while coarser ones in the upper stream (highland) areas (Gómez and Kavzoglu 2005; Erenet et al. 2016). In addition, climate and vegetation cover also vary with elevation. In this study, elevation was classified into four classes of 1212–1729 m, 1729–2118 m, 2118–2492 m, and 2492–3046 m. In the third elevation class (2118–2492 m), the probability of landslide occurrence is higher (Fig. 5d) due to the steep slope and the presence of several springs. In the study area, there were no sufficient rain gauge stations.

Proximity to stream/river is an important factor in this study as rivers and streams cause gully erosion and landslides. The landslides due to gully erosion were found in Layo Tirga, Menena, Done, Sula, and Morede areas. Consequently, there are several shallow and deep-seated landslides in these areas. All the way from the apex to the mouth of streams, there is slope toe erosion and saturation of the geological material thereby increasing its weight. These stream erosions have created small gully to large gorges thereby causing small shallow

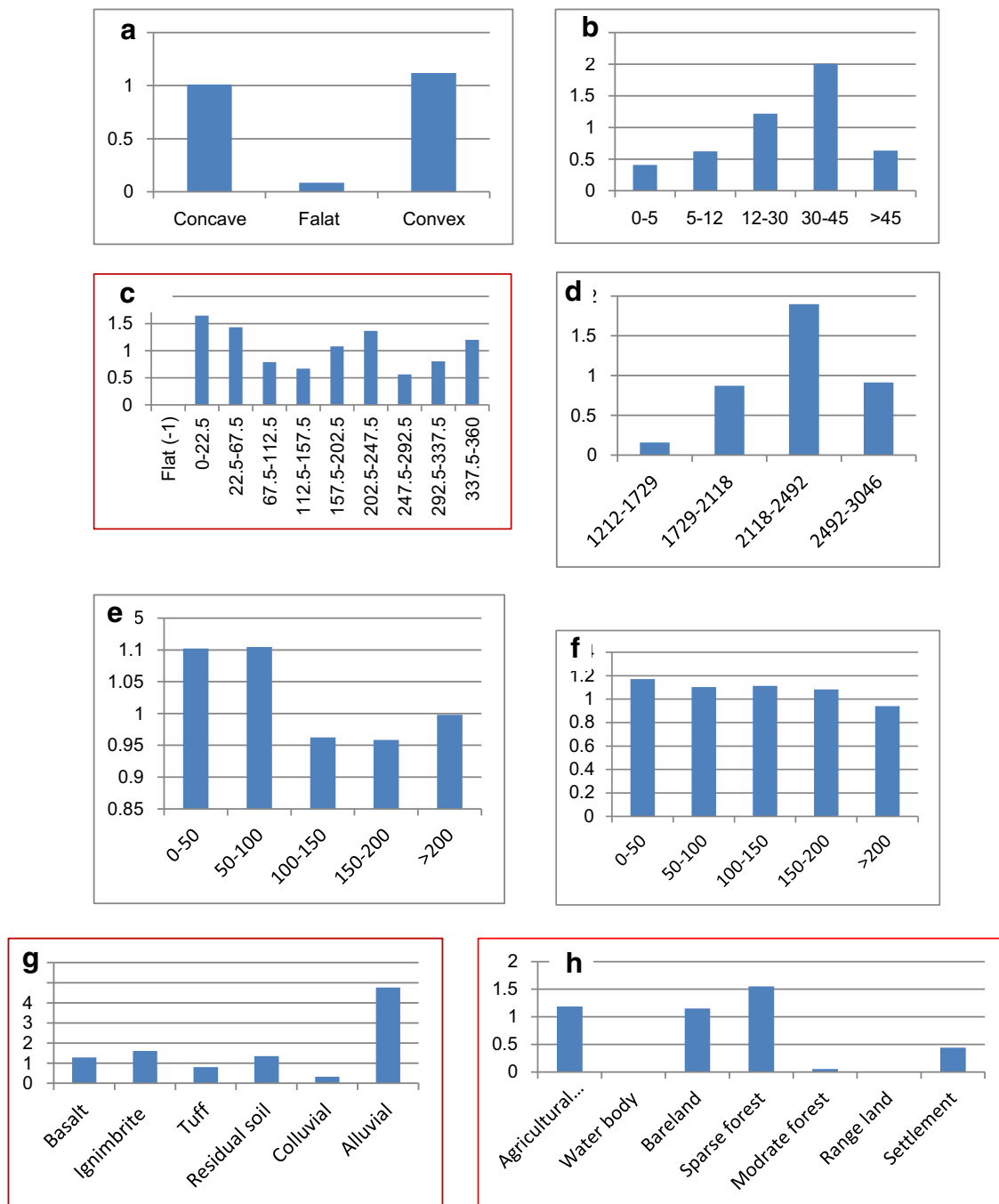


Fig. 5 Frequency ratio value of each factor class: **a** curvature, **b** slope, **c** aspect, **d** elevation, **e** proximity to stream, **f** proximity to lineament, **g** geological units, and **h** land use/land cover

landslides with very short run-out distance and gorges with large-scale landslides respectively. Large streams in the area cause slope instability and carry sediments to rift valley (flat land) or to the flat land at bottom of fault scars. As described in different literatures (Benda and Dunne 1997; Korup et al. 2004; Schuerch et al. 2006; Fuller et al. 2016; Shu et al. 2019), a landslide is the main source of sediments in mountainous terrains. Among the five classes of proximity to streams ranging from 0 to 50 m and 50 to 100 m are the most

influencing ones in causing landslides (Fig. 5e) as these caused slopes undercutting, increment of moisture within geological materials, and fluctuation of groundwater level.

Groundwater is the most important factor which affects or initiates deep-seated landslides in the present study area. This was identified in the field, a number of springs were visible at the bases of failure surface of active landslides and as well as the location of old landslides also with different volumes of discharges. Field observation showed that most of the deep-

seated landslides were caused by groundwater conditions. Some of the springs in this study area are flowing through rock fractures and others are discharged between the contacts of soils and rocks. Landslides due to groundwater are found in different land use/land cover areas.

The environment of rock and soil formation, its composition, compaction, weathering, etc. affect slope instability as these have an impact on the strength of geological materials which resulted in uneven landscape modification (Fig. 4). Ground modifications are affecting human activities. Landslide is one of the ground modification processes which affect human lives and their day-to-day activities. The lithologic units in the study area include basalt, ignimbrite, tuff, alluvial soil, colluvial soil, and residual soil. From rock units, basalts and ignimbrite are the dominant rock units in the study area based on their areal coverage (Fig. 3g). In ignimbrite rock, various sized landslides such as rockfalls and rock slides were found in the south, east, and central parts of the study area. The landslides observed in basaltic rocks are debris and a few rock slides.

Geological structures considered in this study were megascopic structures or tectonic structures. Tectonic structures are buffered based on the effect of these structures. As the distance from the fault/lineament increases, the number of landslides decreased. In the fault area, the crushing of rocks increases but the strength of rocks decreases. This fault zone is also an area where many springs are emanating near the fault line. In addition to the north-south oriented major faults, there are some fractures oriented to the same directions with the major fault with small distortion. The buffering analysis of lineaments/faults and fractures/ produced the distance to lineament classes of 0–50 m, 50–100 m, 100–150 m, 150–200 m, and > 200 m in which the first four classes have a significant contribution to landslide occurrence (Fig. 5f).

The final landslide susceptibility map was produced by combining the 8 landslide conditioning factors that are listed in Fig. 5. Then, the predicted probability values have been classified into five susceptibility classes of 0–0.2, 0.2–0.4, 0.4–0.6, 0.6–0.8, and > 0.8 for very low, low, moderate, high, and very high susceptibility classes respectively with their corresponding area coverage of 17.83%, 29.19%, 28.54%, 17.52%, and 6.91%.

Model validation and evaluation

The receiver operating characteristic (ROC) curve was used to evaluate the prediction performance of the landslide susceptibility model (Shano et al. 2020). The model validation is the most important step which was applied before the write-up of the interpretation of the model. There are different types of landslide susceptibility or hazard model validation methods if models were produced by the statistical, multi-criteria decision, and artificial intelligence. These are density overlying,

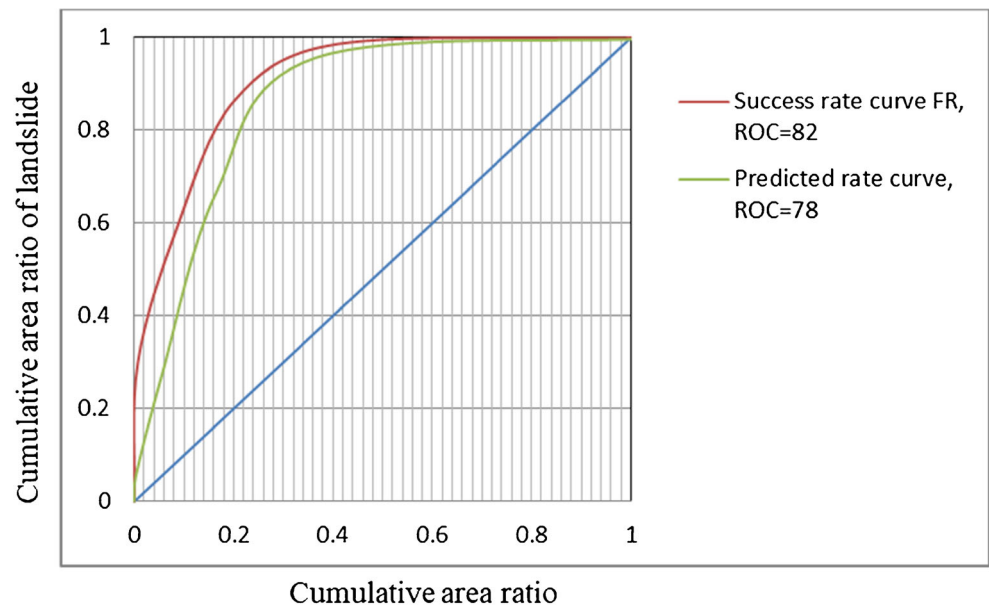
field observation, success rate curve, and receiver operator characteristic curve (Zhou et al. 2002; Shano et al. 2020). Although this step is very important, it has not scientifically tested AUC value assignment from ROC (Chung and Fabbri 2003). A receiver operating characteristic (ROC) curve plots the true positive rate (sensitivity) against the false-positive rate (1–specificity) (Zhou et al. 2002; Baeza et al. 2009; Krzanowski and Hand 2009; Shano et al. 2020). Generally, as sensitivity increases, specificity also increases. The current research was to evaluate the landslide susceptibility model by using a receiver operating characteristic (ROC) curve and this was supported by field observation. The result of AUC which is indicated in Fig. 6 shows that the success curve is 82% and the predicate rate curve is 78%.

Discussion

In this study for the frequency ratio model, eight predisposing factors were selected. The causative factors selected for landslide susceptibility mapping were slope, aspect, curvature, elevation, proximity to stream, proximity to lineament, lithology, and land use/land cover. Although the spatial distribution of rainfall map of the area was not prepared due to the small area nature and less number of well-distributed rain gauge stations of the current study area, rainfall is still considered as a triggering factor. These selected factors can be grouped into four categories, i.e., morphometric, hydrological, geological, and land use/land cover. Accordingly, these factors will be discussed one by one in the following paragraphs as to why and how they are influencing the landslide susceptibility in their different classes. The first group is DEM derivative or morphometric factors, for example, slope, aspect, curvature, and elevation. The result of the frequency ratio in Fig. 5 (a–h) indicates the degree of each factor class's influence towards landslide occurrence. Among the five slope classes, the two classes (i.e., 12–30° and 30–45°) have a frequency ratio value greater than 1 which shows their high degree of influence in causing landslides (Fig. 5b). As these slope classes are covered by soil and highly weathered rock units, highly affected by gully erosion and agricultural activities, and have high concentration of springs as well as geological structures/lineaments, many landslides occurred. These two slope classes are the most landslide-prone sections that need remedial measures to reduce landslide hazards.

The slope aspect has ten classes among which five classes (i.e., north, northeast, south, southwest, and north) have the highest degree of influence on landslide occurrence (Fig. 5c). This is because slope aspect controls slopes' exposure to sunlight, wind, and rainfall. Due to these conditions, the moisture content increases within geological materials. Curvature has three classes in which two of them are more influential on landslide occurrence and their frequency ratio values are

Fig. 6 ROC curve of frequency ratio



greater than one. This is due to groundwater accumulated in concave curvature while erosion is active in convex curvature. Soil mass and/or highly weathered rock units were visible in these types of the area. When coming to elevation, it has also a great influence on the slope instability. Once the elevation in the study area increases, the rainfall amount also increases. Due to different types of vegetation and the high amount of rainfall at higher elevations, the area has thick soil with high moisture content. Because of these factors, landslides are occurring more frequently in the higher elevation than at the lower elevation (Fig. 5d).

Geological units that affected the present study area are lithology and soil types. The parameters included under this factor are basalt, ignimbrite, tuff, colluvial soil, alluvial soil, and residual soil. Most of the landslides are concentrated on basalt, ignimbrite, residual, and alluvial soils. This is because the basaltic rock unit covered the steep slope parts of the study area; it is highly affected by tectonic structures. Springs with different volumes of discharge are found along these geological structures and presence of deep local weathering. So that landslide distribution concentrated along and around fault zones. Ignimbrite is the second abundant lithology in the study area in which some fault scars are exposed at the lower part of the flat land. The landslide types observed on this rock unit are some rock slides and rock block fails. Alluvial and residual soils are the soil types in which landslides are frequently found (Fig. 5g). The number of landslides which were found on alluvial and residual soils has exceptionally very high-frequency ratio values. This is due to erosion activity of the streams on alluvial soils and due to intense cultivation, high groundwater occurrence, and steep slope in residual soils.

The proximity factors used for landslide susceptibility mapping are proximity to lineament and stream/river erosion.

The tectonic structures are buffered outward from the imaginary center line to 200 m far away from the center. As the frequency ratio model indicated, landslide density is decreasing from an imaginary center line to 200 m. This is because the rocks around the fault zone are highly fractured and deeply weathered as well as plenty of springs along the fault zones. Besides, some of the streams flow along these tectonic lineaments. The second proximity factor was stream erosion which has a great influence on landslide occurrences. To characterize their influence on landslide were buffered in the distances of 0–50 m, 50–100 m, 100–150 m, 150–200 m, and greater than 200 m. These classes were ranged based on the influence of stream on landslide occurrence. In the first class or near the banks of streams, there are a number of landslides that have been occurred due to toe erosion, increasing weight of geological materials, and decreasing the shear strength. These landslides are characterized at initial points of the stream where there were shallow landslides and averagely the sizes are increasing in the flow direction of streams. This is because the stream size increase as the size of the gully also increases and initiated large landslides.

The hydrological factors include groundwater level and rainfall. To discuss groundwater, there was subsurface data limitation. However, based on the field surveys, most of the deep-seat landslides which are the depth of failure surface greater than 5 m were caused by groundwater. The cardinal evidence observed in the field is that springs at the base of the failure surface and around different corners of the failure surface. The landslides of the area are triggered by prolonged and heavy rainfall. The high prolonged and heavy rainfall of the area mostly occurred in the months of April, May, September, and October; the monthly rainfall is greater than 170 mm.

Land use/land cover of the area has seven classes including agricultural land, settlement, bare land, rangeland, water body, sparse forest, and moderate forest. From these classes, landslides are most frequently found on agricultural land and loose/sparse forest classes. Relatively several numbers of landslides were also encountered in sparse forest areas of the study area. Vegetation covers can either promote a landslide (which is a negative effect) or control a landslide (which is a positive effect). The frequency ratio indicated that forest cover of this specific area has a positive effect. In addition, the area with sparse forest is more affected by landslides than the area with moderate forest. Due to hydrological and mechanical effects, forest covers reduce landslide occurrences. In the hydrological processes, plants absorb water through roots and reduce the water content in the void spaces of soil grains and rock fractures. Plants with long roots are connecting together the geological materials below and above the failure surface thereby increasing the shear strength of geological materials.

The main advantage of frequency ratio model is that each input parameter is compared independently with the landslides training map. This preformed the pixels of a class of reclassified factor map and the pixels of reclassified landslide training map independently calculated and the percentage of training class over the percentage of a class of factor map is known as frequency ratio. Due to this advantage, frequency ratio analysis is applied in this study independently. The values of each input parameter are simply added by using map algebra in the ArcGIS environment in the final compilations of the resulting landslide susceptibility map was map produced.

When the researcher read the landslide susceptibility map, there are different colors and naming of the landslide susceptibility map (Fig. 7). The naming in this map has its meaning based on the conformation of the real observation in the field. The name of the susceptibility zone and the description are represented in Table 2.

Fig. 7 Landslide susceptibility map

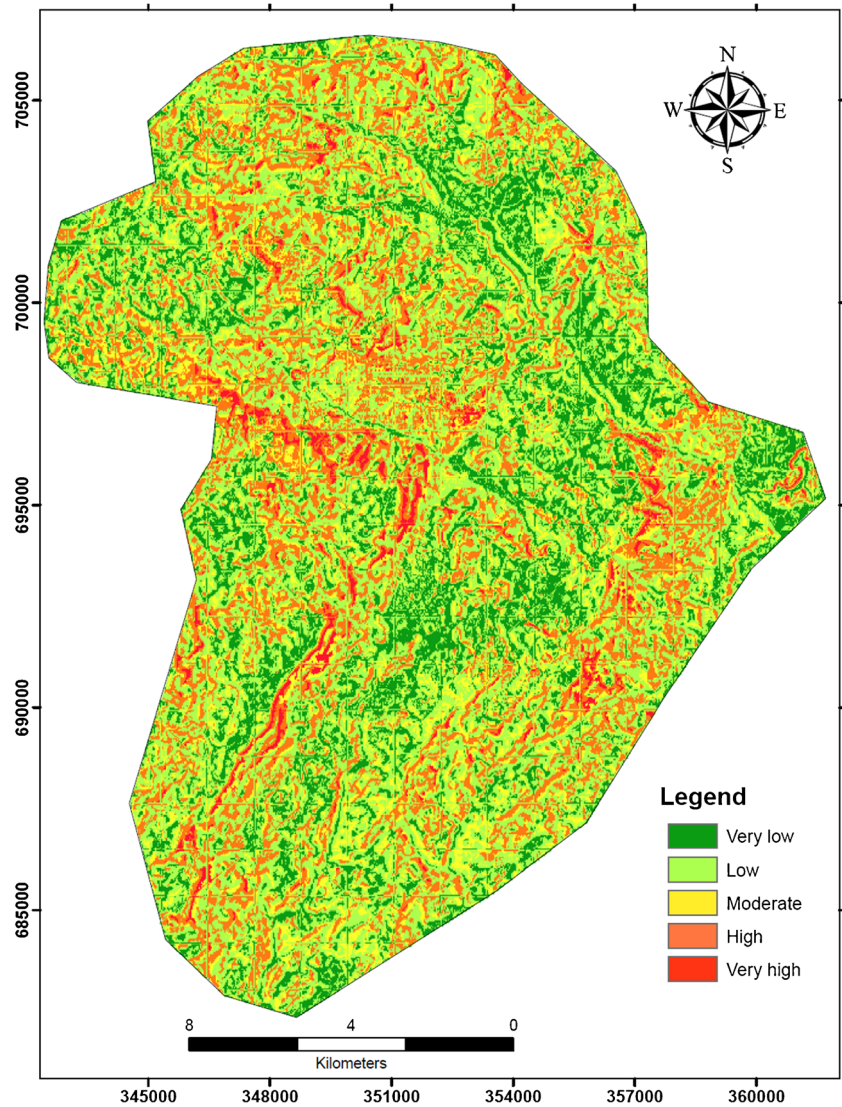


Table 2 Description of each zone in the landslide susceptibility map

Susceptibility classes	Descriptor	Total pixel =312,579		Landslide distribution in each class	Description
		No of pixels	% area coverage		
Very low	Rare	55,742	17.83202	6	The event is conceivable, but only under exceptional circumstances
Low	Unlikely	91,253	29.19209	51	The event might occur under very adverse circumstances
Moderate	Possible	89,233	28.54588	124	The event could occur under adverse conditions
High	Likely	54,755	17.51628	273	The event will probably occur under adverse conditions
Very high	Almost certain	21,596	6.90862	1100	The event is expected to occur

Conclusion

The results from the frequency ratio model indicated that with different thematic factors, there were various classes with their own influences on landslide occurrence. The slope class has five classes among which two classes of 12–30° and 30–45° have a significant impact on landslide occurrence as they have frequency ratio values of 1.22 and 2.01 respectively. The contribution of land use/land cover in facilitating landslides in these slope classes was very high. From frequency ratio model analysis, the slope curvature, both convex and concave shaped classes also contributed significantly in initiating landslides. This thematic layer has more influence on the soil and highly weathered basalt of the study area. These convex and concave classes are related to groundwater and stream erosion. Aspect is also one basic factor initiating landslides in the study area in which the north, northeast, southeast, south, and southwest are the main influencing aspect classes. Elevation has also an indirect influence on landslide occurrence. Geological units are consisting of rocks and soils found in the study area and they have a tremendous influence on landslide occurrence. The proximity to lineament classes of 0–50 m, 50–100 m, 100–150 m, and 150–200 m and land use/cover classes of sparse forest, barren land, and agricultural land have a significant contribution to landslide occurrence. The frequency ratio model of landslide hazard zonation in the present study area is most applicable for factor-class-based remedial measures. Based on the frequency ratio model, all eight factors have their own clear influence on landslide occurrence. Therefore, to minimize landslide occurrence of the area better to take action on these factors or evacuate the local settlers.

Acknowledgements The first author expresses sincere thanks to the Addis Ababa Science and Technology University and Arba Minch University for giving an opportunity to pursue this Ph.D. study. Also, the author has special thanks to Dr. Abate Demissie (Department of foreign language and literature, ArbaMinch University) for the detailed editing of this research paper. Last but not least, Mr. Belachew Mogos, Leta Gudissa, and Tilahun Mersha for their support during research work.

Code availability Not applicable.

Declarations

Conflict of interest The author declares no competing interests.

References

- Abdulwahid WM, Pradhan B (2017) Landslide vulnerability and risk assessment for multi-hazard scenarios using airborne Laser Scanning Data (LiDAR). *Landslides* 14:1057–1076
- Abija FA, Nwosu JI, Ifedotun AI, Osadebe CC (2019) Landslide susceptibility assessment of Calabar, Nigeria using geotechnical, remote sensing and multi-criteria decision analysis: implications for urban planning and development. *SDRP J Earth Sci Environ Stud* 4:774–788. <https://doi.org/10.25177/jeses.4.6.ra.617>
- Ada M, San BT (2017) Comparison of machine-learning techniques for landslide susceptibility mapping using two-level random sampling (2LRS) in Alakir catchment area, Antalya, Turkey. *Nat Hazards* 90:237–263
- AGS (Australian Geomechanics Society) (2000) Landslide risk management concepts and guidelines. Australian Geomechanics Society, Subcommittee on Landslide Risk Management. *Australian Geome* 35:49–92
- Akgün A, Bulut F (2007) GIS-based landslide susceptibility for Arsin-Yomra (Trabzon, North Turkey) region. *Environ Geol* 51:1377–1387. <https://doi.org/10.1007/s00254-006-0435-6>
- Aleotti P, Chowdhury R (1999) Landslide hazard assessment: summary review and new perspectives. *Bull Eng Geol Environ* 58:21–44. <https://doi.org/10.1007/s100640050066>
- Ayalew L (1999) The effect of seasonal rainfall on landslides in the highlands of Ethiopia. *Bull Eng Geol Environ* 58:9–19. <https://doi.org/10.1007/s100640050065>
- Ayalew L, Yamagishi H (2004) Slope failures in the Blue Nile basin, as seen from landscape evolution perspective. *Geomorphology* 57(1–2):95–116
- Baeza C, Lantada N, Moya J (2009) Influence of sample and terrain unit on landslide susceptibility assessment at La Pobla de Lillet, Eastern Pyrenees, Spain. *Environ Earth Sci* 60:155–167
- Benda L, Dunne T (1997) Stochastic forcing of sediment supply to channel networks from landsliding and debris flow. *Water Resour Res* 33:2849–2863. <https://doi.org/10.1029/97wr02388>
- Berhane G, Kebede M, Alfarah N, Hagos E, Grum B, Giday A, Abera T (2020) Landslide susceptibility zonation mapping using GIS-based frequency ratio model with multi-class spatial data-sets in the Adwa-Adigrat mountain chains, northern Ethiopia. *J Afr Earth Sci* 164: 103795. <https://doi.org/10.1016/j.jafrearsci.2020.103795>

- Budimir MEA, Atkinson PM, Lewis HG (2015) A systematic review of landslide probability mapping using logistic regression. *Landslides* 12:419–436. <https://doi.org/10.1007/s10346-014-0550-5>
- Carrara A, Cardinali M, Detti R, Guzzetti F, Pasqui V, Reichenbach P (1991) GIS techniques and statistical models in evaluating landslide hazard. *Earth Surf Proc Landfor* 16:427–445
- Carrara A, Cardinali M, Guzzetti F, Reichenbach P (1995) GIS technology in mapping landslide hazard. *Adv Nat Technol Hazards Res.* https://doi.org/10.1007/978-94-015-8404-3_8
- Catani F, Casagli N, Ermini L, Righini G, Menduni G (2005) Landslide hazard and risk mapping at catchment scale in the Arno River basin. *Landslides* 2:329–342. <https://doi.org/10.1007/s10346-005-0021-0>
- Chen W, Shahabi H, Shirzadi A, Hong H, Akgun A, Tian Y et al (2018) Novel hybrid artificial intelligence approach of bivariate statistical-methods-based kernel logistic regression classifier for landslide susceptibility modeling. *Bull Eng Geol Environ* 78:4397–4419
- Chimidi G, Raghuvanshi TK, Suryabagavan KV (2017) Landslide hazard evaluation and zonation in and around Gimbi town, western Ethiopia—a GIS-based statistical approach. *Appl Geoma* 9:219–236
- Chowdhury M, Sadek AW (2012) Advantages and limitations of artificial intelligence. *Transport Res Circular E-C168*.
- Chung CJF, Fabbri AG (2003) Validation of spatial prediction models for landslide hazard mapping. *Nat Hazards* 30:451–472. <https://doi.org/10.1023/b:nhaz.0000007172.62651.2b>
- Ciurleo M, Cascini L, Calvello M (2017) A comparison of statistical and deterministic methods for shallow landslide susceptibility zoning in clayey soils. *Eng Geol* 223:71–81. <https://doi.org/10.1016/j.enggeo.2017.04.023>
- Dagdelenler G, Ercanoglu M, Sonmez H (2020) Semi-automatic landslide inventory mapping with multiresolution segmentation process: a case study from Ulus District (Bartın, NW Turkey). *ICL Cont to Landslide Disaster Risk Reduc.* https://doi.org/10.1007/978-3-030-60227-7_8
- Dahl MPJ, Mortensen LE, Veihe A, Jensen NH (2010) A simple qualitative approach for mapping regional landslide susceptibility in the Faroe Islands. *Nat Hazards Earth Syst Sci* 10:159–170. <https://doi.org/10.5194/nhess-10-159-2010>
- Donati L, Turrini M (2002) An objective method to rank the importance of the factors predisposing to landslides with the GIS methodology: application to an area of the Apennines (Valnerina; Perugia, Italy). *Eng Geol* 63:277–289. [https://doi.org/10.1016/s0013-7952\(01\)00087-4](https://doi.org/10.1016/s0013-7952(01)00087-4)
- Duman TY, Çan T, Emre Ö, Keçer M, Doğan A, Ateş Ş, Durmaz S (2005) Landslide inventory of northwestern Anatolia, Turkey. *Eng Geol* 77:99–114. <https://doi.org/10.1016/j.enggeo.2004.08.005>
- Erener A, Düzgün HSB (2011) Landslide susceptibility assessment: what are the effects of mapping unit and mapping method? *Environ Earth Sci* 66:859–877. <https://doi.org/10.1007/s12665-011-1297-0>
- Erener A, Mutlu A, Sebnem Düzgün H (2016) A comparative study for landslide susceptibility mapping using GIS-based multi-criteria decision analysis (MCDA), logistic regression (LR) and association rule mining (ARM). *Eng Geol.* <https://doi.org/10.1016/j.enggeo.2015.09.007>
- Fell R, Corominas J, Bonnard C, Cascini L, Leroi E, Savage WZ (2008) Guidelines for landslide susceptibility, hazard and risk zoning for land use planning, on behalf of the JTC-1 Joint Technical Committee on Landslides and Engineered Slopes. *Eng Geol* 102:85–98
- Fuller IC, Riedler RA, Bell R, Marden M, Glade T (2016) Landslide-driven erosion and slope–channel coupling in steep, forested terrain, Ruahine Ranges, New Zealand, 1946–2011. *CATENA* 142:252–268
- Gómez H, Kavzoglu T (2005) Assessment of shallow landslide susceptibility using artificial neural networks in Jabonosa River Basin, Venezuela. *Eng Geol* 78:11–27. <https://doi.org/10.1016/j.enggeo.2004.10.004>
- Guzzetti F, Carrara A, Cardinali M, Reichenbach P (1999) Landslide hazard evaluation: a review of current techniques and their application in a multi-scale study, Central Italy. *Geomorphology* 31:181–216
- Guzzetti F, Cardinali M, Reichenbach P, Carrara A (2000) Comparing landslide maps: a case study in the Upper Tiber River basin, Central Italy. *Environ Manag* 25:247–263. <https://doi.org/10.1007/s002679910020>
- Guzzetti F, Reichenbach P, Cardinali M, Galli M, Ardizzone F (2005) Probabilistic landslide hazard assessment at the basin scale. *Geomorphology* 72:272–299. <https://doi.org/10.1016/j.geomorph.2005.06.002>
- Guzzetti F, Reichenbach P, Ardizzone F, Cardinali M, Galli M (2006) Estimating the quality of landslide susceptibility models. *Geomorphology* 81:166–184. <https://doi.org/10.1016/j.geomorph.2006.04.007>
- Guzzetti F, Mondini AC, Cardinali M, Fiorucci F, Santangelo M, Chang KT (2012) Landslide inventory maps: new tools for an old problem. *Earth-Sci Revi* 112:42–66. <https://doi.org/10.1016/j.earscirev.2012.02.001>
- Hong H, Xu C, Bui DT (2015) Landslide susceptibility assessment at the Xiushui area (China) using frequency ratio model. *Procedia Earth Planetary Sci* 15:513–517. <https://doi.org/10.1016/j.proeps.2015.08.065>
- Hu Q, Zhou Y, Wang S, Wang F (2020) Machine learning and fractal theory models for landslide susceptibility mapping: Case study from the Jinsha River Basin. *Geomorphology* 351:106975. <https://doi.org/10.1016/j.geomorph.2019.106975>
- Jager S, Wieczorek GE (1994) Landslide susceptibility in the Tully Valley area, Finger Lakes region, New York. Open-File Report. <https://doi.org/10.3133/ofr94615>
- Kalantar B, Ueda N, Saeidi V, Ahmadi P (2020a) Application of machine learning algorithms and their ensemble for landslide susceptibility mapping. *ICL Con to Landslide Disas Risk Red.* https://doi.org/10.1007/978-3-030-60227-7_25
- Kalantar B, Ueda N, Saeidi V, Ahmadi K, Halin AA, Shabani F (2020b) Landslide susceptibility mapping: machine and ensemble learning based on remote sensing big data. *Remote Sens* 12. <https://doi.org/10.3390/rs12111737>
- Kavzoglu T, Colkesen I, Sahin E K (2018) Machine learning techniques in landslide susceptibility mapping: a survey and a case study. *Adv Nat Technol Hazards Res.* https://doi.org/10.1007/978-3-319-77377-3_13
- Khan H, Shafique M, Khan MA, Bacha MA, Shah SU, Calligaris C (2019) Landslide susceptibility assessment using frequency ratio, a case study of northern Pakistan. *Egypt J Remote Sens Space Sci* 22:11–24
- Korup O, McSaveney MJ, Davies TR (2004) Sediment generation and delivery from large historic landslides in the Southern Alps, New Zealand. *Geomorphology* 61:189–207. <https://doi.org/10.1016/j.geomorph.2004.01.001>
- Krušić J, Marjanović M, Samardžić-Petrović M, Abolmasov B, Andrejev K, Miladinović A (2017) Comparison of expert, deterministic and Machine Learning approach for landslide susceptibility assessment in Ljubovija Municipality, Serbia. *Geofizika* 34:251–273. <https://doi.org/10.15233/gfz.2017.34.15>
- Krzanowski W J, Hand D J (2009) ROC curves for continuous data. <https://doi.org/10.1201/9781439800225>
- Lee CT (2015) Review and perspectives on methodology for landslide hazard analysis: 10th Asian Regional conference of IAEG (2015).
- Lee S, Min K (2001) Statistical analysis of landslide susceptibility at Yongin. *Korean Environ Geol* 40:1095–1113
- Li Y, Chen W (2019) Landslide susceptibility evaluation using hybrid integration of evidential belief function and machine learning techniques. *Water*. <https://doi.org/10.3390/w12010113>
- Mahmood I, Qureshi SN, Tariq S, Atique L, Iqbal MF (2015) Analysis of landslides triggered by October 2005, Kashmir Earthquake. *PLOS Curr Disaster.* <https://doi.org/10.1371/currents.dis.0bc3ebc5b8adf5c7fe9fd3d702d44a99>
- Malamud BD, Turcotte DL, Guzzetti F, Reichenbach P (2004) Landslide inventories and their statistical properties. *Earth Surf Proc Landfor* 29:687–711. <https://doi.org/10.1002/esp.1064>

- Mersha T, Meten M (2020) GIS-based landslide susceptibility mapping and assessment using bivariate statistical methods in Simada area, northwestern Ethiopia. *Geoenviron Disas* 7. <https://doi.org/10.1186/s40677-020-00155-x>
- Meten M, PrakashBhandary N, Yatabe R (2015) Effect of landslide factor combinations on the prediction accuracy of landslide susceptibility maps in the Blue Nile Gorge of Central Ethiopia. *Geoenviron Disaster* 2. <https://doi.org/10.1186/s40677-015-0016-7>
- Murillo-García FG, Alcántara-Ayala I, Ardizzone F, Cardinali M, Fiorucci F, Guzzetti F (2014) Erratum to: Satellite stereoscopic pair images of very high resolution: a step forward for the development of landslide inventories. *Landslides* 12:293–293. <https://doi.org/10.1007/s10346-014-0525-6>
- Neuhäuser B, Terhorst B (2007) Landslide susceptibility assessment using “weights-of-evidence” applied to a study area at the Jurassic escarpment (SW-Germany). *Geomorphology* 86:12–24
- Nguyen V, Pham B, Vu B, Prakash I, Jha S, Shahabi H, Shirzadi A, Ba D, Kumar R, Chatterjee J, Tien Bui D (2019) Hybrid machine learning approaches for landslide susceptibility modeling. *Forests*. 10. <https://doi.org/10.3390/f10020157>
- Nhu VH, Mohammadi A, Shahabi H, Ahmad BB, Al-Ansari N, Shirzadi A, Clague JJ, Jaafari A, Chen W, Nguyen H (2020) Landslide susceptibility mapping using machine learning algorithms and remote sensing data in a tropical environment. *Int J Environ Res Public Health* 17. <https://doi.org/10.3390/ijerph17144933>
- Pal SC, Chowdhuri I (2019) GIS-based spatial prediction of landslide susceptibility using frequency ratio model of Lachung River basin, North Sikkim, India. *SN Appl Sci* 1. <https://doi.org/10.1007/s42452-019-0422-7>
- Park S, Kim J (2019) Landslide susceptibility mapping based on random forest and boosted regression tree models, and a comparison of their performance. *Appl Sci* 9. <https://doi.org/10.3390/app9050942>
- Pradhan B (2013) A comparative study on the predictive ability of the decision tree, support vector machine and neuro-fuzzy models in landslide susceptibility mapping using GIS. *Comput Geosci* 51:350–365
- Pradhan B, Buchroithner MF (2010) Comparison and validation of landslide susceptibility maps using an artificial neural network model for three test areas in Malaysia. *Environ Eng Geosci* 16:107–126
- Pradhan B, Lee S (2009) Delineation of landslide hazard areas on Penang Island, Malaysia, by using frequency ratio, logistic regression, and artificial neural network models. *Environ Earth Sci* 60:1037–1054
- Pradhan B, Lee S, Buchroithner MF (2010) Remote sensing and GIS-based landslide susceptibility analysis and its cross-validation in three test areas using a frequency ratio model. *Photogrammetrie - Fernerkundung - Geoinformation* 2010:17–32. <https://doi.org/10.1127/1432-8364/2010/0037>
- Raghuvanshi TK, Ibrahim J, Ayalew D (2014) Slope stability susceptibility evaluation parameter (SSEP) rating scheme – an approach for landslide hazard zonation. *J Afr Earth Sci* 99:595–612
- Rahardianto T, Saputra A, Gomez C (2017) Assessment of landslide distribution map reliability in Niigata prefecture – Japan using frequency ratio approach. <https://doi.org/10.1063/1.4987086>
- Reichenbach P, Rossi M, Malamud BD, Mihir M, Guzzetti F (2018) A review of statistically-based landslide susceptibility models. *Earth-Sci Rev* 180:60–91. <https://doi.org/10.1016/j.earscirev.2018.03.001>
- Riaz MT, Basharat M, Hameed N, Shafique M, Luo J (2018) A data-driven approach to landslide-susceptibility mapping in mountainous terrain: case study from the Northwest Himalayas. *Pakistan Nat Hazards Rev* 19:05018007. [https://doi.org/10.1061/\(asce\)nh.1527-6996.0000302](https://doi.org/10.1061/(asce)nh.1527-6996.0000302)
- Ruff M, Czurda K (2008) Landslide susceptibility analysis with a heuristic approach in the Eastern Alps (Vorarlberg, Austria). *Geomorphology* 94:314–324
- Sarkar S, Roy AK, Raha P (2016) Deterministic approach for susceptibility assessment of shallow debris slide in the Darjeeling Himalayas, India. *CATENA* 142:36–46. <https://doi.org/10.1016/j.catena.2016.02.009>
- Schuerch P, Densmore AL, McArdell BW, Molnar P (2006) The influence of landsliding on sediment supply and channel change in a steep mountain catchment. *Geomorphology* 78:222–235. <https://doi.org/10.1016/j.geomorph.2006.01.025>
- Shano L, Raghuvanshi TK, Meten M (2020) Landslide susceptibility evaluation and hazard zonation techniques – a review. *Geoenviron Disas* 7. <https://doi.org/10.1186/s40677-020-00152-0>
- Shu H, Hürlimann M, Molowny-Horas R, González M, Pinyol J, Abancó C, Ma J (2019) Relation between land cover and landslide susceptibility in Val d’Aran, Pyrenees (Spain): historical aspects, present situation and forward prediction. *Sci of The Total Environ* 693:133557. <https://doi.org/10.1016/j.scitotenv.2019.07.363>
- Silalahi FES, Pamela AY, Hidayat F (2019) Landslide susceptibility assessment using frequency ratio model in Bogor, West Java, Indonesia. *Geosci Let* 6. <https://doi.org/10.1186/s40562-019-0140-4>
- Stanley T, Kirschbaum DB (2017) A heuristic approach to global landslide susceptibility mapping. *Nat Hazards* 87:145–164. <https://doi.org/10.1007/s11069-017-2757-y>
- Taylor F, Brabb E E (1986) Map showing the status of landslide inventory and susceptibility mapping in California. Open-File Report. <https://doi.org/10.3133/ofr86100>
- Van Asch TW, Buma J, Van Beek LP (1999) A view on some hydrological triggering systems in landslides. *Geomorphology* 30:25–32. [https://doi.org/10.1016/s0169-555x\(99\)00042-2](https://doi.org/10.1016/s0169-555x(99)00042-2)
- Van Westen CJ, van Asch TWJ, Soeters R (2005) Landslide hazard and risk zonation—why is it still so difficult? *Bull Eng Geol Environ* 65:167–184. <https://doi.org/10.1007/s10064-005-0023-0>
- Van Westen CJ, Castellanos E, Kuriakose SL (2008) Spatial data for landslide susceptibility, hazard, and vulnerability assessment: an overview. *Eng Geol* 102:112–131
- Van Westen C J, Ghosh S, Jaiswal P, Martha T R, Kuriakose S L (2013) From landslide inventories to landslide risk assessment: an attempt to support methodological development in India. *Landslide Sci Pract* https://doi.org/10.1007/978-3-642-31325-7_1
- Varnes D, IAEG (1984) Landslide hazard zonation: a review of principles and practice. U N Sci Cult Organ, Paris, pp 1–6
- Wang X, Liu J, Wang Y, Bi J (2009) Visualization of spatial-temporal data based on 3D virtual scene. *Int Symp Spatial Anal*. <https://doi.org/10.1117/12.838626>
- Wang Q, Li W, Chen W, Bai H (2015) GIS-based assessment of landslide susceptibility using certainty factor and index of entropy models for the Qianyang County of Baoji city, China. *J Earth Syst Sci* 124:1399–1415. <https://doi.org/10.1007/s12040-015-0624-3>
- Wang Z, Liu Q, Liu Y (2020) Mapping landslide susceptibility using machine learning algorithms and GIS: a case study in Shexian County, Anhui Province, China. *Symmetry* 12. <https://doi.org/10.3390/sym12121954>
- Weirich F, Blesius L (2007) Comparison of satellite and air photo based landslide susceptibility maps. *Geomorphology* 87:352–364. <https://doi.org/10.1016/j.geomorph.2006.10.003>
- Wubalem A (2021) Landslide susceptibility mapping using statistical methods in Uatza catchment area, northwestern Ethiopia. *Geoenviron Disaster* 8. <https://doi.org/10.1186/s40677-020-00170-y>
- Wubalem A, Meten M (2020) Landslide susceptibility mapping using information value and logistic regression models in Goncha Siso Eneses area, northwestern Ethiopia. *SN Appl Sci* 2. <https://doi.org/10.1007/s42452-020-2563-0>
- Zhou C, Lee C, Li J, Xu Z (2002) On the spatial relationship between landslides and causative factors on Lantau Island, Hong Kong. *Geomorphology* 43:197–207. [https://doi.org/10.1016/s0169-555x\(01\)00130-1](https://doi.org/10.1016/s0169-555x(01)00130-1)